

# Excess Enthalpies for (Water + Methane)

## Vapor up to 698.2 K and 12.6 MPa

A new flow mixing calorimeter has been used to make measurements of the excess enthalpy of water vapor + methane at temperatures up to 698.2 K and pressures up to 12.62 MPa. Tests on the calorimeter and consistency tests on the measurements suggest that the results are free from significant error. The measurements are fitted to an equation from which excess volumes and compressibility factors for the mixture are calculated.

C. J. WORMALD and  
C. N. COLLING

School of Chemistry  
The University  
Bristol, England

### SCOPE

While volumetric methods are the principal source of thermodynamic information on vapor mixtures, the large adsorption error which occurs when measurements on mixtures containing water vapor are attempted severely limit the accuracy obtainable. For binary mixtures measurement of the excess enthalpy is an alternative to measurement of the excess volume. Excess enthalpy measurements made in a continuous flow mixing calorimeter are quite free from adsorption error. A low-pressure flow mixing calorimeter has already been used to make measurements on some binary mixtures containing water vapor. Analysis of the results yielded accurate cross-term second virial coefficients  $B_{12}$  for water + nitrogen, + hydrogen, + methane, and + argon in the range 373 to 423 K. A new high-pressure flow

mixing calorimeter has been constructed and used to make excess enthalpy measurements on water + methane up to 698.2 K and pressures of 12.62 MPa. Extrapolation of the measurements to low pressures shows that the new high-pressure calorimeter yields results which are in excellent agreement with results obtained using the well-tested low-pressure calorimeter. Using a single value of the excess volume at 698.2 K obtained from the Peng-Robinson equation of state as a constant of integration, thermodynamic analysis of the excess enthalpy measurements yields good values of the excess volume and compressibility factors for the mixture over the entire temperature and pressure range.

### CONCLUSIONS AND SIGNIFICANCE

A new flow calorimetric technique for the measurement of the excess enthalpy of vapors at high temperatures and pressures has been developed. Tests on the calorimeter show that heat leaks are negligible. Excess enthalpies obtained using the calorimeter are in excellent agreement with results obtained on a well-tested low-pressure mixing calorimeter. The overall ac-

curacy of the excess enthalpies is 2%. Thermodynamic analysis of the measurements yields accurate excess volumes and compressibility factors. The new flow mixing calorimeter yields thermodynamic data which are free from adsorption error, and makes possible the study of highly polar fluid mixtures.

### INTRODUCTION

Compression experiments on mixtures containing water vapor have failed to yield accurate or reproducible results. Adsorption errors are large, particularly at pressures approaching saturation and at temperatures below the critical for water. Cross-term second virial coefficients  $B_{12}$  obtained from compression experiments are usually too negative. Compression experiments have, however, yielded the phase boundaries of several water + hydrocarbon mixtures (Brölls, Peter and Schneider, 1970; Rebert and Kay, 1959). At temperatures below 373 K cross-term second virial coefficients for mixtures containing water have been obtained from measurements of the solubility of water in compressed gases (Rigby and Prausnitz, 1968; Coan and King, 1971). This method is free from adsorption errors and does not require an accurate knowledge of the second virial coefficient of water.

An alternative to pVT is to measure the excess enthalpy  $H^E$ . This quantity can be related to volumetric properties by simple thermodynamics. Measurements of  $H^E$  for water vapor, + nitrogen, + argon, + hydrogen and + methane at temperatures to 423.15 K and at pressures in the region of atmospheric have been reported (Richards, Wormald and Yerlett, 1981; Richards and Wormald, 1981). These measurements were made using a carefully tested mixing calorimeter (Wormald, 1977). Excess volumes and  $B_{12}$ 's derived from  $H^E$  measurements on n-alkanes have been

shown (Hutchings, Lewis and Wormald, 1978, 1979) to be in close agreement with the best available volumetric measurements (Dantzler, Knobler and Windsor, 1968). Low-pressure  $H^E$  measurements for water + methane (Smith, Sellars, Yerlett and Wormald, 1983) have been shown to yield  $B_{12}$ 's in good agreement with those obtained from solubility measurements of Rigby and Prausnitz (1968).

A new flow mixing calorimeter designed for operation at pressures up to 14 MPa and temperatures up to approximately 700 K has been constructed and used to make measurements on a number of mixtures containing water vapor. Preliminary accounts of this work have been given (Wormald and Colling, 1979, 1980, 1982) and results of high-pressure measurements on water vapor + nitrogen will be published shortly (Wormald and Colling, 1983).

### EXPERIMENTAL

The high-pressure flow mixing apparatus is shown in Figure 1. Methane entered the flow system via needle valve 1. Water from reservoir 2 or burette 3 was pumped by metering pump 4 into flash boiler 5 immersed in a fluidized alumina bath 6. Methane and water vapor passed through heat exchange coils 7 and 8 where they were brought to the temperature of a second fluidized bath 9. Mixing occurred in calorimeter 10 over an electrical heater which was adjusted to offset the cooling effect produced

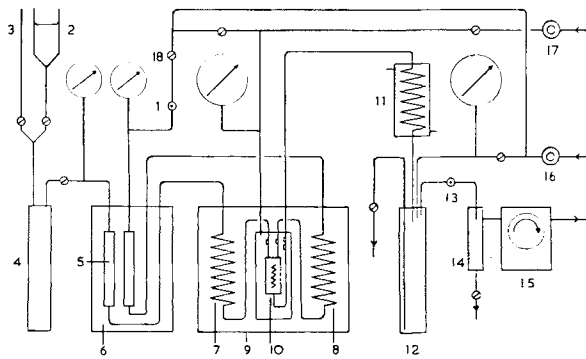


**Figure 1.** The flow calorimetric apparatus. The apparatus consists of the following principal parts. Water from reservoir 2 or burette 3 flows through metering pump 4 into flash vaporizer 5 mounted in fluidized alumina bath 6. Steam and methane pass through heat exchange coils 7 and 8 immersed in fluidized bath 9 which contains mixing calorimeter 10. Vapor is condensed in water cooled coil 11 and collected in reservoir 12. Needle valves 13 and 1 control the methane flow rate. Trap 14 removes water droplets and gas meter 15 indicates the methane flow rate. Pressures are controlled by regulators 16 and 17 which connect to methane and nitrogen cylinders respectively.

on mixing. Platinum resistance thermometers fixed to the inlet and outlet tubes were used to detect temperature changes. The calorimeter was contained in a pressure vessel maintained at the same pressure as the fluids inside the calorimeter. The mixture leaving the calorimeter was condensed at 11 and collected in vessel 12. Methane was allowed to flow through the system by controlling needle valve 13. Water was trapped out at 14, and the flow rate of methane was measured at atmospheric pressure by gas meter 15. A nitrogen cylinder connected to pressure controller 16 pressurized the vessel containing the calorimeter. A methane cylinder connected to pressure controller 17 supplied gas to the mixing calorimeter via valve 18 and needle valve 1. Methane of not less than 99.5% purity was used. Steam was generated from ordinary distilled water. Extensive tests on several flow mixing calorimeters were carried out before a satisfactory design was achieved. Excess enthalpies measured using a flow calorimeter in which heat leaks and other effects are negligible should be independent of flow rate. Measurements of  $H^E$  for water vapor + nitrogen at  $x = 0.5$  and over a range of flow rate are shown in Figure 2. No significant variation of  $H^E$  with flow rate was found. Further details of the apparatus and of the results for water + nitrogen are reported by Wormald and Colling (1983).

## RESULTS

Excess enthalpies for water vapor + methane in the range 373.15 to 423.15 K and at a pressure of 101.325 kPa have been reported (Smith, Sellars, Yerlett and Wormald, 1983). Results of high-pressure measurements at compositions around  $x = 0.5$  and over a range of temperature and pressure are listed in Table 1. The composition dependence of  $H^E$  was investigated at three temperatures, and these results are listed in Table 2. The measurements recorded for each run are temperature  $T$ /K, pressure  $p$ /MPa, flow rate  $f$ /mmol·s<sup>-1</sup>, mole fraction  $x$ , and the power  $P$  supplied to the calorimeter heater to obtain an isothermal state. The quantity  $P/f$  is the excess enthalpy obtained under actual experimental conditions. In any individual run the temperature may have differed by about a degree from the intended temperature and the composition may have differed by about 2% from  $x = 0.5$ . The excess enthalpy  $H^E$ /J·mol<sup>-1</sup> listed in Table 1 was obtained by correcting  $P/f$  to  $x = 0.5$  and to the intended temperature.

The results listed in Table 1 are shown in Figure 3. The solid lines in the figure were calculated using Eq. 24. The lines terminate at the saturation pressure for water. The composition dependence of  $H^E$  is shown in Figure 4. The curves are skewed parabolas with maxima towards the water-rich side.

## THERMODYNAMICS OF GASEOUS MIXTURES

The properties of gases at the densities used in this work can be described using the pressure series form of the virial equation of

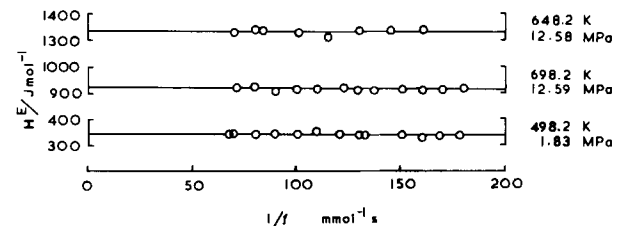


**Figure 2.** Results of heat leak tests on the flow mixing calorimeter using nitrogen + steam. The excess enthalpy at  $x = 0.5$  plotted against reciprocal molar flow rate is flow rate independent.

state truncated after the  $p^4$  term,

$$pV = RT + B'p + C'^2_p + D'^3_p + E'^4_p, \quad (1)$$

where

$$B' = B \text{ and } C' = \frac{(C - B^2)}{RT} \quad (2)$$

Similar equations relating  $D'$  and  $E'$  to the virial coefficients  $B$ ,  $C$ ,  $D$  and  $E$  can be written.

The excess volume  $V^E$  of a binary mixture is defined by the equation

$$V^E = V_m - xV_1 - (1 - x)V_2 \quad (3)$$

where  $V_1$  and  $V_2$  are the molar volumes of the two pure components. At pressures low enough for virial coefficients higher than the second to be neglected the molar volume  $V_m$  of the mixture is given by

$$V_m = \frac{RT}{P} + B_m, \quad (4)$$

where

$$B_m = x^2B_{11} + 2x(1 - x)B_{12} + (1 - x)^2B_{22}. \quad (5)$$

Equation 3 can be written in terms of the second virial coefficients  $B_{11}$  and  $B_{22}$  for the pure components and the cross-term  $B_{12}$

$$V^E = x(1 - x)(2B_{12} - B_{11} - B_{22}). \quad (6)$$

It follows that

$$G^E = \int V^E dp = x(1 - x)p(2B_{12} - B_{11} - B_{22}), \quad (7)$$

and

$$H^E = G^E - T \left( \frac{\partial G^E}{\partial T} \right)_P = x(1 - x)p(2\phi_{12} - \phi_{11} - \phi_{22}), \quad (8)$$

where

$$\phi^o = B - T \frac{dB}{dT}. \quad (9)$$

The quantity  $\phi^o$  is the isothermal enthalpy-pressure coefficient in the limit of zero pressure

$$\phi^o = \left( \frac{\partial H}{\partial P} \right)_T \text{ Lim } p \rightarrow 0. \quad (10)$$

Coefficients  $\phi_{11}^o$  and  $\phi_{22}^o$  may be obtained by direct measurements of the isothermal Joule-Thomson coefficient or by differentiation of an equation fitted to accurate second virial coefficients. Measurements of  $H^E$  at low pressures therefore allow  $\phi_{12}^o$  to be obtained from Eq. 8.  $B_{12}$  may be obtained from  $\phi_{12}^o$  either by using a suitably adjusted pair potential, a corresponding states correlation or by direct integration of Eq. 9.

At the pressures for which the new excess enthalpies have been measured it is adequate to extend the above equations to include coefficients up to  $E'$ , so that

TABLE 1. EXPERIMENTAL EXCESS ENTHALPIES  $H^E$  FOR WATER VAPOR + METHANE MEASURED OVER A RANGE OF PRESSURE AT SELECTED TEMPERATURES AND AT  $x = 0.5$ 

$\frac{T}{K}$	$x_{\text{H}_2\text{O}}$	$f$ $\text{mmol}\cdot\text{s}^{-1}$	$P$ $\text{J}\cdot\text{s}^{-1}$	$P/f$ $\text{J}\cdot\text{mol}^{-1}$	$p$ $\text{MPa}$	$H^E$ $\text{J}\cdot\text{mol}^{-1}$
$T = 448.2 \text{ K}$						
451.1	0.505	6.711	0.645	96.1	0.35	98.5
451.1	0.501	6.756	1.208	178.8	0.65	183.8
451.6	0.503	6.729	1.825	271.2	0.93	281.0
$T = 473.2 \text{ K}$						
473.8	0.501	7.993	0.722	90.3	0.52	90.9
473.8	0.500	8.034	1.614	200.9	0.93	202.0
473.8	0.501	8.041	2.593	322.5	1.34	324.4
$T = 498.2 \text{ K}$						
495.9	0.499	6.792	0.759	111.7	0.60	110.0
496.2	0.499	6.785	1.344	198.1	1.05	195.0
496.5	0.501	6.763	2.058	304.3	1.55	299.7
496.2	0.500	6.772	2.809	414.8	2.02	406.3
496.1	0.502	6.753	3.829	567.0	2.51	553.9
$T = 523.2 \text{ K}$						
523.8	0.499	7.878	0.871	110.5	0.79	111.0
523.8	0.498	8.028	1.730	215.5	1.48	215.8
523.8	0.499	8.026	2.839	353.7	2.17	355.6
523.8	0.500	8.018	4.051	505.2	2.86	508.2
523.8	0.499	8.044	5.585	694.3	3.58	698.9
$T = 548.2 \text{ K}$						
544.4	0.500	6.778	0.739	109.0	0.8	106.7
544.3	0.502	6.743	1.348	199.9	1.55	194.7
545.1	0.501	5.041	2.073	411.2	2.86	400.9
544.9	0.504	6.733	2.792	414.6	2.93	403.2
544.9	0.503	6.746	4.427	657.5	4.21	635.8
549.1	0.498	8.083	6.998	865.8	4.98	874.0
545.1	0.499	6.802	6.732	989.7	5.55	945.3
$T = 573.2 \text{ K}$						
573.6	0.500	7.986	0.694	86.9	0.86	87.1
573.9	0.497	8.035	1.875	233.3	2.15	234.5
573.7	0.498	9.000	3.827	425.1	3.55	426.9
573.7	0.496	8.071	5.365	664.7	5.00	664.7
573.8	0.498	8.012	7.573	945.2	6.33	946.1
572.0	0.499	8.012	10.29	1284	7.77	1260
$T = 598.2 \text{ K}$						
595.6	0.501	6.762	0.516	76.3	0.80	75.3
595.5	0.501	6.765	1.365	201.8	2.16	198.6
595.7	0.502	6.751	2.389	353.8	3.53	348.0
599.2	0.498	8.038	4.197	522.2	4.89	526.0
595.9	0.503	6.743	3.641	539.9	5.00	530.7
599.1	0.497	8.015	5.873	732.8	6.27	738.1
596.1	0.500	6.785	4.965	731.7	6.31	719.0
599.3	0.501	8.000	7.910	988.8	7.69	998.4
599.1	0.501	7.978	10.51	1317	9.20	1329
598.2	0.502	7.992	13.38	1674	10.44	1674
598.1	0.498	7.896	13.42	1699	10.51	1698
$T = 648.2 \text{ K}$						
647.9	0.497	6.817	0.653	95.8	1.41	95.7
647.9	0.498	6.813	1.304	191.4	2.82	191.1
647.3	0.502	5.037	1.082	214.8	2.86	214.5
648.1	0.497	6.835	2.114	309.3	4.27	309.0
648.2	0.495	6.854	2.919	427.1	5.65	425.7
647.5	0.498	8.002	4.614	576.6	6.86	574.1
648.0	0.494	6.876	3.763	547.2	7.06	547.0
647.5	0.496	8.036	6.055	753.4	8.44	750.0
647.6	0.500	7.990	7.381	923.8	9.79	919.9
647.5	0.497	6.874	6.533	950.4	10.03	945.7
650.4	0.500	6.825	6.529	956.6	10.51	972.8
648.0	0.496	8.043	9.023	1122	11.31	1120
648.1	0.498	7.969	10.797	1355	12.62	1354
$T = 698.2 \text{ K}$						
698.9	0.503	7.991	0.604	75.6	1.55	75.8
699.0	0.499	7.981	1.284	160.9	2.82	161.4
699.0	0.500	7.959	2.075	260.7	4.20	261.6
698.9	0.504	8.021	2.822	351.8	5.69	352.8
699.0	0.500	7.913	3.511	443.7	7.03	445.5
699.2	0.504	8.014	4.532	565.5	8.38	568.4
699.5	0.501	7.884	5.331	676.2	9.82	680.9
699.3	0.505	8.080	6.319	782.0	11.13	787.0
699.2	0.498	7.921	7.298	921.3	12.58	926.8

TABLE 2. MEASUREMENTS OF THE EXCESS ENTHALPY  $H^E$  AT FIXED TEMPERATURE AND PRESSURE MADE OVER A RANGE OF COMPOSITION

$\frac{T}{K}$	$x_{H_2O}$	$\frac{f}{\text{mmol s}^{-1}}$	$\frac{P}{\text{J s}^{-1}}$	$\frac{P/f}{\text{J mol}^{-1}}$	$\frac{H^E}{\text{J mol}^{-1}}$
$T = 548.2 \text{ K}, p = 4.98 \text{ MPa}$					
549.2	0.300	8.107	5.539	683.2	690.9
549.3	0.402	8.066	6.552	812.3	821.1
549.1	0.498	8.083	6.998	865.8	874.9
549.1	0.598	8.002	6.916	864.3	873.0
549.0	0.698	7.927	6.170	778.4	786.0
$T = 598.2 \text{ K}, p = 10.44 \text{ MPa}$					
598.5	0.302	7.946	10.17	1280	1284
598.6	0.399	8.095	12.17	1503	1508
598.2	0.502	7.992	13.38	1674	1679
598.3	0.598	7.980	13.52	1694	1699
598.2	0.698	7.996	12.08	1511	1515
$T = 648.2 \text{ K}, p = 10.51 \text{ MPa}$					
651.4	0.296	6.914	5.394	780.1	800.0
651.7	0.397	6.893	6.189	897.9	920.4
650.4	0.500	6.825	6.529	956.6	980.2
650.0	0.603	6.914	6.667	964.3	986.8
649.9	0.711	6.757	5.569	824.2	843.5

$$\begin{aligned}
 H^E = p & \left\{ \left( B_m - \frac{TdB_m}{dT} - x \left( B_{11} - \frac{TdB_{11}}{dT} \right) \right. \right. \\
 & \left. \left. - (1-x) \left( B_{22} - \frac{TdB_{22}}{dT} \right) \right\} \right. \\
 & + \frac{P^2}{2} \left\{ \left( C'_m - \frac{TdC'_m}{dT} \right) - x \left( C'_{111} - \frac{TdC'_{111}}{dT} \right) \right. \\
 & \left. \left. - (1-x) \left( C'_{222} - \frac{TdC'_{222}}{dT} \right) \right\}. \quad (11)
 \end{aligned}$$

plus similar expressions for the  $D'$  and  $E'$  terms multiplied by  $(p^3/3)$  and  $(p^4/4)$  respectively. This equation is equivalent to Eq. 13 in the paper by Klein, Bennett and Dodge (1971). The first term in Eq. 11 can be rearranged to give Eq. 8. The  $p^2/2$  term can be written in the form

$$\frac{p^2}{2} \{ \dots \} = - \left( \frac{p^2}{RT} \right) (B_m \phi_m^o - x B_{11} \phi_{11}^o - (1-x) B_{22} \phi_{22}^o) \quad (12)$$

$$+ \left( \frac{p^2}{RT} \right) (\psi_m - x \psi_{111} - (1-x) \psi_{222}), \quad (13)$$

where

$$\phi_m^o = x^2 \phi_{11}^o + 2x(1-x) \phi_{12}^o + (1-x)^2 \phi_{22}^o, \quad (14)$$

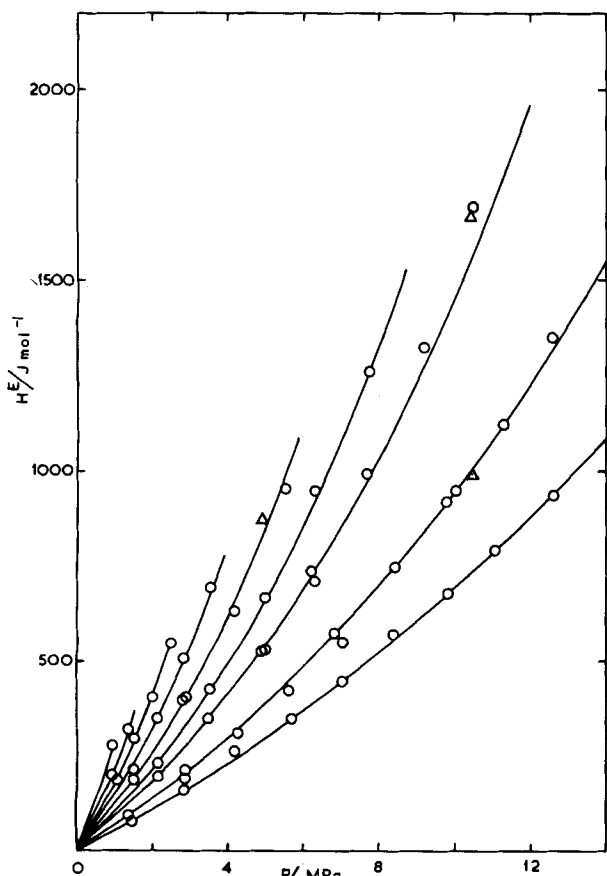


Figure 3. The excess enthalpy of water vapor + methane at  $x = 0.5$  measured over a range of temperature and pressure.  $\circ$ , data listed in Table 1.  $\Delta$ , interpolated from measurements listed in Table 2. Solid lines were calculated from Eq. 24.

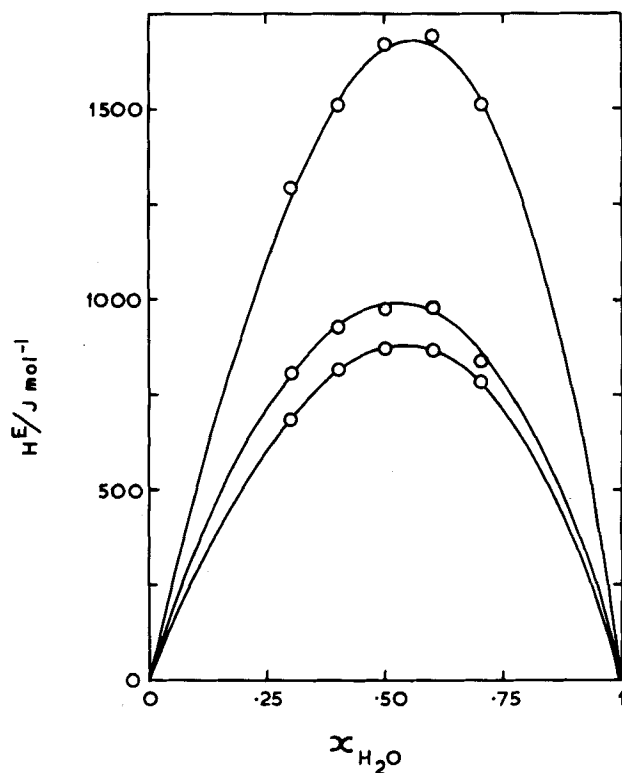


Figure 4. The composition dependence of  $H^E$  for water vapor + methane. The measurements were made at 548.2 K and 4.98 MPa (lower curve), 648.2 K and 10.51 MPa (middle curve), and 598.2 K and 10.44 MPa (upper curve). Interpolation of these data to  $x = 0.5$  gives the values of  $H^E$  shown by the triangles in Figure 3.

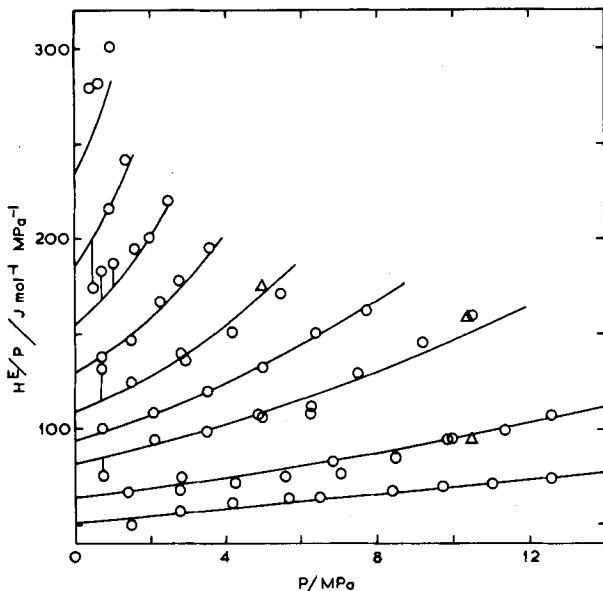


Figure 5. Plot of  $H^E/p$  against  $p$  for water vapor + methane at  $x = 0.5$ . Solid lines are calculated from Eq. 24. The intercepts and initial slopes of the lines are in accord with Eqs. 19 and 20.  $\circ$ , Table 1.  $\Delta$ , interpolated to  $x = 0.5$  from data in Table 2.

$$\psi_m = x^3\psi_{111} + 3x^2(1-x)\psi_{112} + 3x(1-x)^2\psi_{122} + (1-x)^3\psi_{222}, \quad (15)$$

and

$$\psi = C - \frac{T}{2} \frac{dC}{dT}. \quad (16)$$

Equation 11 can be written in the form

$$H^E = \alpha p + \beta p^2 + \gamma p^3 + \delta p^4, \quad (17)$$

where  $\alpha$  is given by Eq. 8,  $\beta$  is the sum of Eqs. 12 and 13 and  $\gamma$  and  $\delta$  are functions of the temperature related to virial coefficients up to  $D$  and  $E$  respectively.

#### THERMODYNAMIC TESTS ON THE $H^E$ MEASUREMENTS

Excess enthalpies obtained using the low-pressure mixing calorimeter have been shown to be consistent with independent thermodynamic measurements but there are no similar data with which the results of the high-pressure experiments may be compared. However, it is possible to see if the measurements obtained using the high-pressure calorimeter are consistent, at least in the low-pressure limit, with results from the low-pressure calorimeter. This comparison is best made by plotting the high-pressure measurements on a graph of  $H^E/p$  against  $p$  as shown in Figure 5. Now Eq. 17 can be written

$$\frac{H^E}{p} = \alpha + \beta p + \gamma p^2 + \delta p^3. \quad (18)$$

If the  $H^E$  measurements are accurate the intercept  $\alpha$  on the plot of  $H^E/p$  against  $p$  should be given by Eq. 8

$$\alpha = x(1-x)(2\phi_{12}^o - \phi_{11}^o - \phi_{22}^o). \quad (19)$$

Neglecting third and higher virial coefficients the initial slope  $\beta$  should be given by

$$\beta = -\left(\frac{p}{RT}\right)(B_m\phi_m^o - xB_{11}\phi_{11}^o - (1-x)B_{22}\phi_{22}^o). \quad (20)$$

Analysis of low-pressure  $H^E$  measurements on water + nitrogen, + argon, and + methane showed that  $B_{12}$ 's and  $\phi_{12}^o$ 's for the water + nonpolar component interaction can be calculated from pure component parameters using the Lennard-Jones or Kihara po-

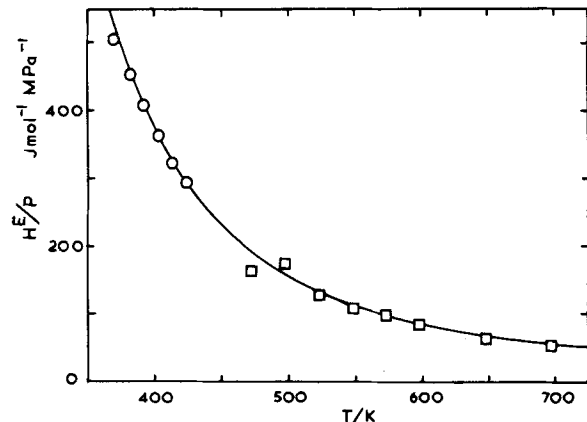


Figure 6. Plot of  $(H^E/p)$  Lim  $p \rightarrow 0$  against  $T$  for water vapor + methane at  $x = 0.5$ . The solid line is calculated from Eq. 19 using Eq. 21 to calculate  $\phi_{12}^o$ .  $\circ$ , obtained from measurements using a low pressure mixing calorimeter.  $\square$ , obtained from measurements listed in Table 1.

tentials for the nonpolar component and the Stockmayer potential for water together with the modified geometric mean rule

$$\epsilon_{12} = 0.85(\epsilon_{11}\epsilon_{22})^{1/2}. \quad (21)$$

Equation 21 has been shown to fit the  $B_{12}$ 's to within experimental error at least between 320 and 450 K. The solid line shown in Figure 6 was calculated using Eq. 19 assuming Eq. 21 is not seriously in error at temperatures up to 698.2 K. As the main contribution to the enthalpy departure arises from interactions between water molecules any inadequacy of Eq. 21 at high temperatures is unlikely to be significant. The circles shown in the lefthand side of Figure 6 are the values of  $(H^E/p)$  Lim  $p \rightarrow 0$  obtained from measurements using the low-pressure mixing calorimeter (Wormald et al., 1983). The squares are the values of  $(H^E/p)$  obtained by extrapolating the measurements made using the high-pressure calorimeter to zero pressure. It can be seen from Figure 5 that the uncertainty on the high-pressure points is less than that at low pressures where  $H^E$  is small. At temperatures below 500 K, where the measurements extend over a short pressure range, the uncertainty on the values of  $H^E/p$  is large. Above 500 K, agreement between the observed intercepts and Eq. 19 is good. These tests, taken together with the flow rate tests shown in Figure 2, suggest that the high-pressure measurements are free from significant error.

#### FITTING THE MEASUREMENTS TO AN EQUATION

As the measurements described in this work are at moderate densities and as the results shown in Figure 5 are monotonic curves we chose to fit the values of  $H^E$  at  $x = 0.5$  listed in Table 1 to Eq. 18 rather than a cubic equation of the van der Waals type. Inspection of plots of  $\ln \alpha$  and  $\ln \beta$  against  $T^{-1}$  suggested that  $\alpha$  and  $\beta$  could best be represented either by equations of the form

$$\alpha(T), \beta(T), \dots = \exp\left(a + \frac{b}{T}\right), \quad (22)$$

or

$$\alpha(T), \beta(T), \dots = \exp\left(a + \frac{b}{T} + \frac{c}{T^2}\right). \quad (23)$$

When Eq. 22 was used for  $\alpha$ ,  $\beta$ ,  $\gamma$  and  $\delta$  the inclusion of a  $p^3$  term in Eq. 18 was essential if the measurements were to be fitted adequately. However when Eq. 23 was used an equivalent fit could be obtained using terms up to  $p^2$  only. This more flexible form was therefore chosen.

Agreement between Eq. 19 and the experimental intercepts shown in Figure 6 is so close that the first coefficient of Eq. 18 was obtained by fitting values of  $\alpha$  calculated from Eqs. 19 and 21 to

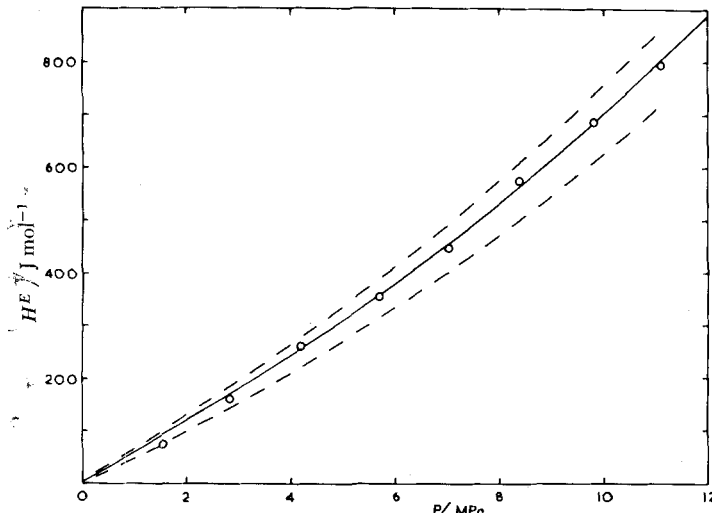


Figure 7. Comparison of  $H^E(x = 0.5)$  at 698.2 K with Peng-Robinson equation of state. The upper broken line was calculated using  $k_{ij} = 0.6$ , the lower broken line using  $k_{ij} = 0.4$ , and the solid line through the points using  $k_{ij} = 0.52$ . O, Table 1.

Eq. 23. Agreement between the initial slopes of lines drawn through the data shown in Figure 5 and Eq. 20 is good but not perfect. Rather than obtain an equation for  $\beta$  by least squares fitting the experimental initial slopes, we chose to calculate values of  $\beta$  using Eq. 21 and 20, and fit these calculated values to Eq. 23. When results of high-pressure measurements of  $H^E$  for water + hydrogen and water + argon have been reported an analysis of the third virial coefficient contribution to  $\beta$  will be undertaken, and improved coefficients for Eq. 23 will be obtained.

Having fitted the  $\alpha$  and  $\beta$  terms the  $\gamma$  term was used as a catch all, and no attempt was made to relate it to virial coefficients. As the results at 373.15 K and 0.101 MPa suggest that the  $\gamma p^2$  term is very small at this pressure, the coefficients of Eq. 23 used to represent the  $\gamma$  term were adjusted to give a value of  $\gamma p^2$  at 373.2 K of less than half the experimental error on these measurements.

The equation to which the measurements were fitted is

$$\frac{H^E}{p} = \sum_{n=1}^{n=3} p^{(n-1)} \exp \left( a_n + \frac{b_n}{T} + \frac{c_n}{T^2} \right), \quad (24)$$

where

$$\begin{aligned} a_1 &= 8.432 \times 10^{-1}, & a_2 &= -5.386, & a_3 &= -2.788 \times 10, \\ b_1 &= 2.338 \times 10^3, & b_2 &= 4.361 \times 10^3, & b_3 &= 2.166 \times 10^4, \\ c_1 &= -1.226 \times 10^5, & c_2 &= -1.895 \times 10^5, & c_3 &= -3.495 \times 10^6. \end{aligned}$$

Equation 24 fits the low-pressure measurements reported previously and the high-pressure measurements listed in Table 2 to within experimental error. The solid lines in Figures 3 and 5 were calculated using this equation. The only data points in Figure 3 not fitted by Eq. 24 are the measurements at 598.2 K at pressures above 9 MPa. It is not clear if these points are slightly too high, or if a better equation than Eq. 24 is needed.

## EXCESS VOLUMES AND COMPRESSIBILITY FACTORS

The excess enthalpy  $H^E$  is related to the excess volume  $V^E$  through

$$\frac{dH^E}{dp} = V^E - T \left( \frac{\partial V^E}{\partial T} \right)_p \quad (25)$$

Integration of Eq. 25 gives

$$V_2^E = T_2 \left[ \frac{V_1^E}{T_1} - \int_{T_1}^{T_2} \frac{(dH^E/dp)}{T^2} dT \right]_p, \quad (26)$$

where  $V_1^E$  and  $V_2^E$  are excess volumes at temperatures  $T_1$  and

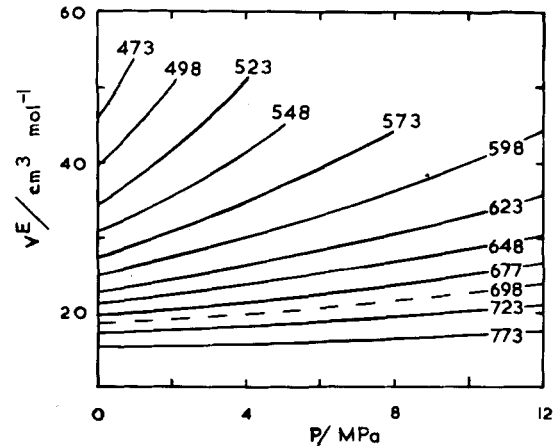


Figure 8. Excess volumes  $V^E$  for water vapor + methane. The broken line at 698.2 K was calculated using the Peng-Robinson equation of state with  $k_{ij} = 0.52$ . These 698.2 K values were used as integration constants in Eq. 26 from which the solid lines were calculated by numerical integration.

$T_2$ .

The best temperature  $T_1$  at which to obtain a value of the integration constant  $V_1^E$  is 698.2 K. At this temperature the degree of association in steam is least,  $V_1^E$  has its smallest value, and the effect on  $V_2^E$  of any uncertainty in  $V_1^E$  is minimized. At high pressures, and in the absence of information about virial coefficients higher than the second, an equation of state other than the virial must be used to obtain  $V_1^E$ . The chosen equation should be capable of giving a good fit to both the residual volume and enthalpy of the two pure components of the mixture. While this is difficult to achieve, the chances of success are greater at 698.2 K than at any lower temperature. A good fit to the excess enthalpy measurements at 698 K can be obtained using the Peng-Robinson equation of state together with the combining rule

$$a_{ij} = (1 - k_{ij})(a_{ii}a_{jj})^{1/2}. \quad (27)$$

Figure 7 shows experimental values of  $H^E$  at  $x = 0.5$  and  $T = 698.2$  K compared with lines calculated from the Peng-Robinson equation using  $k_{ij} = 0.4$ , 0.52 and 0.6. The fit obtained with pure component parameters calculated from criticality conditions and using  $k_{ij} = 0.52$  is to within experimental error. The corresponding values of  $V^E$  at  $x = 0.5$  and  $T = 698.2$  K are shown by the broken line in Figure 8. The intercept  $V_1^E$  at  $p = 0$  is  $18.4 \text{ cm}^3 \cdot \text{mol}^{-1}$ . Equations 6 and 21 yield  $14.5 \text{ cm}^3 \cdot \text{mol}^{-1}$  for the low-density limit. Agreement is as good as can be expected.

The solid lines shown in Figure 8 are the values of  $V^E$  computed using Eqs. 24 and 26. As there is no analytical solution to the exponential term in Eq. 23 a numerical integration technique was used. The value of  $V_1^E$  calculated from the Peng-Robinson equation and used as integration constants in Eq. 26 are listed at the foot of Table 3.

Compressibility factors at  $x = 0.5$  were calculated from

$$Z = \frac{p(V^E + xV_{11} + (1 - x)V_{22})}{RT} \quad (28)$$

Molar volumes for methane were taken from the 1978 IUPAC tables and from the International Steam Tables for water. Compressibility factors at temperatures up to 773 K are listed in Table 3. The use of an additional term in Eq. 24 to secure a better fit to the  $H^E$  measurements, or the choice of a better equation of state to obtain the integration constant  $V_1^E$  at 698.2 K is unlikely to change the calculated compressibility factors by more than  $2 \times 10^{-4}$ .

## ACKNOWLEDGMENT

The award of a British Gas Scholarship to C. N. Colling is gratefully acknowledged.

TABLE 3. COMPRESSIBILITY FACTORS  $Z \times 10^4$  FOR WATER VAPOR + METHANE AT  $x = 0.5$ 

$p/\text{MPa}$	1	2	3	4	5	6
$T/\text{K}$						
473.2	9,855					
498.2	9,877	9,742				
523.2	9,903	9,799	9,688			
548.2	9,922	9,840	9,756	9,668	9,575	
573.2	9,936	9,872	9,806	9,739	9,670	9,598
598.2	9,947	9,896	9,843	9,790	9,738	9,684
623.2	9,956	9,913	9,872	9,830	9,789	9,749
648.2	9,963	9,928	9,894	9,861	9,829	9,797
673.2	9,969	9,940	9,912	9,885	9,843	9,835
698.2	9,974	9,949	9,926	9,904	9,884	9,864
723.2	9,978	9,957	9,938	9,920	9,903	9,888
748.2	9,981	9,964	9,948	9,933	9,920	9,907
773.2	9,984	9,969	9,957	9,944	9,933	9,924
$p/\text{MPa}$						
$T/\text{K}$	7	8	9	10	11	12
573.2	9,520	9,430				
598.2	9,629	9,572	9,508	9,434	9,344	
623.2	9,708	9,668	9,626	9,582	9,536	9,483
648.2	9,766	9,736	9,705	9,675	9,645	9,531
673.2	9,811	9,788	9,766	9,745	9,724	9,703
698.2	9,791	9,828	9,812	9,798	9,696	9,767
723.2	9,873	9,860	9,848	9,837	9,826	9,817
748.2	9,896	9,886	9,876	9,868	9,861	9,876
773.2	9,914	9,907	9,900	9,894	9,889	9,885
Integration Constants $V_1^E/\text{cm}^3 \cdot \text{mol}^{-1}$ Calculated at 698.2 K						
$p/\text{MPa}$	1	2	3	4	5	6
$V_1^E/\text{cm}^3 \cdot \text{mol}^{-1}$	18.8	19.2	19.6	20.0	20.5	20.9
$p/\text{MPa}$	7	8	9	10	11	12
$V_1^E/\text{cm}^3 \cdot \text{mol}^{-1}$	21.3	21.8	22.2	22.7	23.2	23.7

## NOTATION

$a_n$	= coefficient of fitting equation
$a_{ii}$	= coefficient of Peng-Robinson equation
$a_{ij}$	= cross-term coefficient of Peng-Robinson equation
$b_n$	= coefficient of fitting equation
$B = B'$	= second virial coefficient
$c_n$	= coefficient of fitting equation
$C$	= third virial coefficient
$C'$	= third coefficient of pressure series
$D$	= fourth virial coefficient
$D'$	= fourth coefficient of pressure series
$E$	= fifth virial coefficient
$E'$	= fifth coefficient of pressure series
$f$	= molar flow rate
$G^E$	= excess Gibbs function
$H^E$	= excess enthalpy
$k_{ij}$	= combining rule parameters
$p$	= pressure
$P$	= power supplied to heater
$R$	= universal gas constant
$T$	= Kelvin temperature
$V$	= molar volume
$V^E$	= excess volume
$x$	= mole fraction
$Z$	= compressibility factor

## Greek Letters

$\alpha$	= first coefficient of $H^E(p, T)$ equation
$\beta$	= second coefficient of $H^E(p, T)$ equation
$\gamma$	= third coefficient of $H^E(p, T)$ equation
$\delta$	= fourth coefficient of $H^E(p, T)$ equation
$\phi^o$	= isothermal Joule-Thomson coefficient
$\psi$	= defined by Eq. 16
$\epsilon$	= potential well depth

## Subscripts

$i, j$	= components of binary mixture
$m$	= mixture
$n$	= number of term in fitting equation

## LITERATURE CITED

Angus, S., B. Armstrong, and K. M. De Reuck. *International Tables of the fluid state: Methane*, Butterworths, London (1978).

Brölls, K., K. Peter, and G. M. Schneider, "Fluid Mixtures under High Pressure," *Ber. Bunsenges. Phys. Chem.*, **74**, p. 682 (1970).

Coan, C. R., and A. D. King, "Solubility of Water in Compressed Carbon Dioxide, Nitrous Oxide and Ethane," *J. Am. Chem. Soc.*, **93**, p. 1957 (1971).

Dantzler, E. M., C. M. Knobler, and M. L. Windsor, "Interaction Virial Coefficients in Hydrocarbon Mixtures," *J. Phys. Chem.*, **72**, p. 676 (1968).

Hutchings, D. J., E. J. Lewis, and C. J. Wormald, "Excess Enthalpies of Mixtures of Methane + Each of the n-Alkanes from Ethane to n-Octane," *J. Chem. Thermodyn.*, **10**, p. 559 (1978).

Klein, R. F., C. O. Bennett, and B. F. Dodge, "Experimental Heats of Mixing for Gaseous Nitrogen + Methane," *AIChE J.*, **17**, p. 958 (1971).

Richards, P., and C. J. Wormald, "The enthalpy of mixing of (water + argon) vapour," *Z. Phys. Chem. N. F.*, Wiesbaden, **35**, p. 128 (1981).

Le Fevre, E. J., M. R. Nightingale, and J. W. Rose, "The Second Virial Coefficient for Ordinary Water Substance, a New Correlation," *J. Mech. Eng. Sci.*, **17**, p. 243 (1975).

Peng, D., and D. B. Robinson, "A New Two Constant Equation of State," *Ind. Eng. Chem. Fund.*, **15**, p. 59 (1976).

Rebert, C. J., and W. B. Kay, "The Phase Behavior and Solubility Relations of the Benzene-Water System," *AIChE J.*, **5**, p. 285 (1959).

Richards, P., C. J. Wormald, and T. K. Yerlett, "The Excess Enthalpy of (Water + Nitrogen) Vapour and (Water + n-Heptane) Vapour," *J. Chem. Thermodyn.*, **13**, p. 623 (1981).

Rigby, M., and J. M. Prausnitz, "Solubility of Water in Compressed Nitrogen, Argon and Methane," *J. Phys. Chem.*, **72**, p. 283 (1968).

Smith, G., A. Sellars, T. K. Yerlett, and C. J. Wormald, "The Excess Enthalpy of (Water + Hydrogen) Vapour and (Water + Methane) Vapour,"

*J. Chem. Thermod.*, 29, p. 15 (1983).  
 U. K. Steam Tables in S. I. Units, Edward Arnold, London (1970).  
 Wormald, C. J., "A Differential Flow Mixing Calorimeter: The Excess Enthalpy of Methane + Benzene, Methane + Cyclohexane, and Benzene + Cyclohexane," *J. Chem. Thermod.*, 9, p. 901 (1977).  
 Wormald, C. J., "Thermodynamic Properties of Some Mixtures Containing Steam," *Proc. N.P.L. Conf. Fluids and Fluid Mixtures*, I.P.C. Press p. 175 (1978).  
 Wormald, C. J., E. J. Lewis, and D. J. Hutchings, "Excess Enthalpies of Gaseous Mixtures of n-Alkanes," *J. Chem. Thermod.*, 11, p. 1 (1979).  
 Wormald, C. J., and C. N. Colling, "Excess Enthalpies of Some Mixtures Containing Steam," *Proc. 9th Int. Conf. Properties of water and steam*, Pergamon 655 (1979).  
 Wormald, C. J., and C. N. Colling, "Excess Enthalpies of Some Binary Steam Mixtures," *Thermodynamics of Aqueous System with Industrial Application, A.C.S. Symp. Ser.*, 133, p. 435 (1980).  
 Wormald, C. J., and C. N. Colling, "Excess Enthalpy Experimental Data: Binary Systems Water + Hydrogen, Water + Methane, Water + Nitrogen and Water + Argon," *Gas Processors Assoc., Tech. Pub. TP-7*, Tulsa, OK (1982).  
 Wormald, C. J., and C. N. Colling, "Excess Enthalpies for Water Vapour + Nitrogen up to 698.2 K and 12.6 MPa," *J. Chem. Thermod.* 15, p. 725 (1983).

*Manuscript received February 9, 1983; revision received May 17, and accepted May 31, 1983.*

# Gas-Liquid Mass Transfer in Fixed-Bed Reactors with Cocurrent Downflow Operating in the Pulsing Flow Regime

Liquid-side mass transfer coefficients were measured for cocurrent two-phase downflow in 5 and 10 cm diameter columns packed with 2.5 and 4 mm Raschig rings. Experiments were specifically carried out in the pulsing flow regime. The mass transfer coefficients were determined via absorption of CO<sub>2</sub> into buffer solutions with the advantage of a high absorbing capacity. Thus columns of 1 m length could be used. Relations are proposed based on the hydrodynamic phenomena observed in pulsing flow. From these relations a correlation for  $k_L$  is found in terms of flow rates and packing characteristics that satisfies the experimental data.

**J. R. BLOK, C. E. KONING,  
A. A. H. DRINKENBURG**

**Laboratory for Chemical Engineering  
Rijksuniversiteit Groningen  
Groningen, the Netherlands**

## SCOPE

Packed columns with cocurrent downflow of gas, trickle-bed reactors, are often used in industry. Different flow regimes can be distinguished, normally operation is in the so-called gas-continuous regime, where hydrodynamic interaction between gas and liquid is low as in a countercurrently operated column. At higher gas and liquid loads liquid-rich waves travel through the column, pulsing flow. In the pulsing flow regime operation

can be very advantageous, since the degree of axial mixing decreases and the rate of mass transfer between gas and liquid increases.

In this contribution relations are given for the rate of mass transfer between gas and liquid in dependence on gas and liquid velocity and holdup in the pulsing flow regime.

## CONCLUSIONS AND SIGNIFICANCE

It appears possible to explain experimental mass transfer between gas and liquid in pulsing trickle bed reactors with a model that assumes that in pulsing flow two distinct phases of the liquid can be distinguished: the pulses and the regions in between the pulses. Increasing the liquid flow rate means that more pulses appear in the bed, but the regions in between the pulses remain the same in liquid holdup and mass transfer rate per unit volume. Since the holdup and pulse frequencies are known from earlier investigations, we can work out a relation-

ship for the mass transfer coefficient that covers the experimental findings within 20%:

$$k_L a = 5.9 \cdot 10^{-2} \cdot S \epsilon^{-2.2} u_L u_g^{0.58}$$

The results support the concept of pulsing flow being a transition zone between the gas-continuous and the dispersed bubble flow regime, where the pulses are moving zones in the bed, already in the dispersed bubble flow regime, interspersed by gas-continuous zones.

## INTRODUCTION

Packed columns with cocurrent downflow of gas and liquid are widely used in the chemical and especially the petrochemical in-

dustry. One of the main advantages is the fact that high throughput rates are possible for liquid and gas. The disadvantage that only one theoretical mass transfer stage can be attained is generally overcome by a great absorbing capacity in one of the two phases, be it physically or chemically; often the transferred component is consumed by a chemical reaction either directly in the liquid phase or at the catalytic surface of the packing. The overall rate of the

Present address of J. R. Blok: Shell Nederland Chemie b.v., Vondelingenweg 601 3194 AJ Rotterdam-Hoogvliet, The Netherlands.